

On the phase diagram of 1+1D Abelian-Higgs model and its critical point

Titus Chanda,^{1,*} Maciej Lewenstein,^{2,3} Jakub Zakrzewski,^{1,4} and Luca Tagliacozzo⁵

¹*Instytut Fizyki Teoretycznej, Uniwersytet Jagielloński, Lojasiewicza 11, 30-348 Kraków, Poland*

²*ICFO-Institut de Ciències Fotòniques, The Barcelona Institute of Science and Technology,*

Av. Carl Friedrich Gauss 3, 08860 Barcelona, Spain

³*ICREA, Passeig Lluís Companys 23, 08010 Barcelona, Spain*

⁴*Mark Kac Complex Systems Research Center, Jagiellonian University in Krakow, Lojasiewicza 11, 30-348 Kraków, Poland.*

⁵*Departament de Física Quàntica i Astrofísica and Institut de Ciències del Cosmos (ICCUB),*

Universitat de Barcelona, Martí i Franquès 1, 08028 Barcelona, Catalonia, Spain

We investigate in detail the phase diagram of the Abelian-Higgs model in one spatial dimension and time (1+1D) on a lattice. We identify a line of first order phase transitions separating the Higgs region from the confined one. This line terminates in a quantum critical point above which the two regions are connected by a smooth crossover. We analyze the critical point and find compelling evidences for its description as the product of two non-interacting systems, a massless free fermion and a massless free boson. However, we find also some surprising results that cannot be explained by our simple picture, suggesting this newly discovered critical point to be an unusual one.

Introduction.— Gauge theories in 1+1 dimensions (1D in space and time) are ideal playgrounds to characterize the effects of strong-coupling between matter and gauge fields. Many of the non-perturbative aspects of 3+1 dimensional gauge theories relevant to our understanding of particle physics, such as quark confinement and chiral symmetry breaking, have a 1+1D analogue. Furthermore, 1+1D field theories can often be treated analytically [1, 2] providing important insights to the physics of 1+1D systems relevant also to condensed matter physics.

In this work, we study the lattice version of a relativistic bosonic field that interacts with a photonic field [3], the bosonic version of the Schwinger model [4–7]. In contrast to (polarized) fermions, bosons can have contact interactions that are described by the well known Abelian-Higgs model (AHM) in 1+1D (AHM₂) [8–12].

In the AHM₂, non-perturbative effects completely modify the phase diagram from the picture of weak coupling of the bosonic matter to the gauge field [13]. Naively, one would expect to observe two phases characteristic of the Higgs mechanism [8–11], a superfluid phase 1, characterized by the quasi-condensation of bosons (Higgs phase) and a Mott-insulating phase 2, dominated by the strong interactions. However, non-perturbative calculations show that the phenomenology in the phase 1 is the same as in the phase 2, and bosons are always tightly confined [13] (for a recent discussion on a single phase in the continuum see e.g. [14, 15]).

One can indeed certify the presence of a phase transition in $d+1$ dimension for any $d > 2$ [16, 17], but due to the (somewhat boring) expectation of only a single phase in the continuum, the phase diagram of the AHM₂ (without a topological θ term) has never been computed on the lattice in 1+1D. This work thus aims at filling this gap.

Our work is strongly motivated by the current prospects of simulating lattice gauge theories using cold atomic setups [18–23]. In this context, fueled by the fact

that bosons are easier to cool down than fermions that facilitates experimental studies of these systems, the experiments along the lines proposed in [24–30] should soon explore the phase diagram of the AHM₂.

Physicists have been working hard to measure the Higgs mode in experiments with cold atoms for a long-time, as recently reviewed in [31]. In 2+1D, only an explicit particle-hole symmetry protects the decay of the Higgs mode into Goldstone modes, and thus allows a proper measurement of its mass. These conditions are only met at the tip of the lobes of the Mott insulator to superfluid transition in Bose-Hubbard systems [32–34]. Unfortunately, in 1+1D, at the tip of the Mott lobe there is Berezinskii-Kosterlitz-Thouless (BKT) transition (see e.g., [35–38]) that is not particle-hole symmetric. This observation seems to strengthen the picture emerging from the presence of a single phase in AHM₂ and seems to suggest that a proper Higgs mode does not exist in 1+1D.

The results we present here indicate a different picture, still characterized by a single phase, but with a reach landscape of transitions.

By performing numerical simulations of the Hamiltonian version of the AHM₂ based on matrix product states (MPS) [39, 40], we confirm the presence of a single phase for all the values of the mass of the bosons μ^2/q^2 and their interaction strength λ/q^2 , measured in unit of the bosonic charge q in agreement with the field theoretical analysis. However, unexpectedly, for small λ/q^2 we find a line of first order quantum phase transitions (FOQPT) between the “Higgs” and the “confined” regions. This line ends, for a finite value of λ/q^2 , in a critical second order quantum phase transition (SOQPT), above which the two regions are continuously connected through a smooth crossover. Nevertheless, close to the phase transition line the two regions are well separated and we can thus identify a “Higgs” mode and study its behavior as we approach the continuum limit, at least at sufficiently

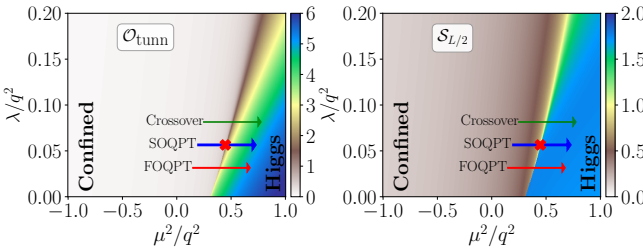


FIG. 1. Phase diagram of the AHM₂ (1) in the $(\mu^2/q^2, \lambda/q^2)$ -plane for a system of linear size $L = 60$. At small couplings, the system may occupy two qualitatively different regions, a confined and an Higgs region. The two regions are separated by a line of FOQPT as witnessed both by the average tunneling amplitude $\mathcal{O}_{\text{tunn}}$ (left panel) (effectively zero in the confined region and finite in the Higgs region) and the entanglement entropy $S_{L/2}$ measured at the center of the chain (right panel) (small in the confined region and large in the Higgs region). The line of FOQPT ends at a SOQPT, above which the two regions are smoothly connected and thus represent different aspects of a single phase.

small λ/q^2 . One can indeed take a different continuum limit to the standard one by approaching, from the Higgs region, the newly discovered SOQPT.

We spend most of our work to precisely identify the position and the nature of the new critical point. By assuming Lorentz invariance at the critical point and using then the machinery of conformal field theories (CFT), we can understand the critical point as the direct sum of two non-interacting fields: a free fermionic field describing the amplitude or Higgs mode and a free bosonic field, a collective mode of the Goldstone modes and the gauge field. As appealing as this picture looks like, there are still surprising results that do not fit with it. As we discuss below, the question of a complete characterization of the nature of the critical point is truly an outstanding challenge.

The model.— Following [3], we discretize the bosonic AHM₂ obtaining the following Hamiltonian on a finite 1D lattice with open boundary conditions, with lattice spacing a containing L sites and $L - 1$ bonds (see [41] for details):

$$\hat{H} = \sum_j \left[\hat{L}_j^2 + 2x \hat{\Pi}_j^\dagger \hat{\Pi}_j + \left(4x - \frac{2\mu^2}{q^2} \right) \hat{\phi}_j^\dagger \hat{\phi}_j + \frac{\lambda}{q^2} (\hat{\phi}_j^\dagger)^2 \hat{\phi}_j^2 - 2x (\hat{\phi}_{j+1}^\dagger \hat{U}_j \hat{\phi}_j + h.c.) \right], \quad (1)$$

with $x = 1/a^2 q^2$. The operators acting on the matter fields $\{\hat{\phi}_j, \hat{\phi}_j^\dagger, \hat{\Pi}_j, \hat{\Pi}_j^\dagger\}$ act in Hilbert space associated to sites j , while the operators acting on gauge-fields $\{\hat{L}_j, \hat{U}_j, \hat{U}_j^\dagger\}$ act in Hilbert spaces defined on bonds connecting two sites, j and $j + 1$. The operators fulfill the standard commutation relations $[\hat{\phi}_j, \hat{\Pi}_k] = [\hat{\phi}_j^\dagger, \hat{\Pi}_k^\dagger] = i\delta_{jk}$, $[\hat{L}_j, \hat{U}_j] = -\hat{U}_j$ and $[\hat{L}_j, \hat{U}_j^\dagger] = \hat{U}_j^\dagger$.

The usual continuum limit entails the limit $x \rightarrow \infty$. Here we fix $x = 2$ and characterize the phase diagram on the lattice.

As usual, we can define creation and annihilation operators for particles ‘ a ’ and anti-particles ‘ b ’ as \hat{a}_j and \hat{b}_j fulfilling $[\hat{a}_j, \hat{a}_k^\dagger] = [\hat{b}_j, \hat{b}_k^\dagger] = \delta_{jk}$ [42]. We perform MPS simulations using the density matrix renormalization group (DMRG) algorithm [39, 40, 43–46] to find the ground state of the above Hamiltonian in the full range of parameters. While in principle the bosonic Hilbert spaces are infinite dimensional, in our simulations, we study the system in the first 11 states, obtained by limit the occupation to at most $n_0^a = n_0^b = 10$ [47].

In absence of external charges, the local U(1) symmetry implies the Gauss law $\hat{G}_j = 0$, $\forall j$, where the generators are [3] $\hat{G}_j = \hat{L}_j - \hat{L}_{j-1} - \hat{Q}_j$, and $\hat{Q}_j = \hat{a}_j^\dagger \hat{a}_j - \hat{b}_j^\dagger \hat{b}_j$ encodes the density of dynamical charges. Using the Gauss law, we can integrate-out the gauge-fields in a chain with open-boundary conditions in favor of a long-range potential for the matter fields [4].

Confined and Higgs, two shades of the same phase.—

The long-range interactions among the bosons completely destroy the two phases of the standard 1+1D Bose Hubbard model. Our numerical results for the phase diagram are presented in Fig. 1 in terms of μ^2/q^2 and λ/q^2 . For $\lambda/q^2 \geq 0$, the system is in the confined region as far as $\mu^2/q^2 \leq 0$. In this region the model has a finite mass gap. Here, the elementary excitations are mesons, bound pairs of particle-antiparticle. The gauge bosons are in the lowest eigenstate of \hat{L}_j , so that the variance $\sigma^2(\hat{L}_j) = \langle \hat{L}_j^2 \rangle - \langle \hat{L}_j \rangle^2 \approx 0$.

For $\mu^2/q^2 \gg 0$, the system enters the Higgs region where the variance $\sigma^2(\hat{L}_j)$ becomes large. The effective gauge-field mediated tunneling amplitude $\mathcal{O}_{\text{tunn}} = \frac{1}{2L} \sum_j \langle \hat{\phi}_{j+1}^\dagger \hat{U}_j \hat{\phi}_j + h.c. \rangle$ increases and can be used as an “order parameter” for the Higgs region.

We can also characterize the two regions by considering the behavior of the entanglement entropy of a block made of l constituents starting from the boundary, defined as

$$S_l = -\text{Tr} [\rho_l \ln \rho_l], \quad (2)$$

where $\rho_l = \text{Tr}_{l+1, l+2, \dots, L} |\psi\rangle \langle \psi|$ is the reduced density matrix. In the Higgs region, the entanglement entropy is systematically larger than in the confined region.

For sufficiently small λ/q^2 , the two regions are separated by a line FOQPT characterized by discontinuous jumps both in the average tunneling amplitude $\mathcal{O}_{\text{tunn}}$ and in the entanglement entropy $S_{L/2}$ measured across the central bond. This line terminates at a critical SOQPT at a finite value of λ_c/q^2 and μ_c^2/q^2 , identified by the red cross in Fig. 1. We discuss precise location and characterization of this critical point below. Above the SOQPT, the two regions are smoothly connected as shown by the fact that all the physical quantities smoothly crossover

from zero to finite values as we move from one region to the other.

Nature of the critical point.— By assuming that the critical point is Lorentz invariant [48], and thus is ultimately described, at low energies, by a CFT, we can precisely locate and characterize it.

In a CFT, the finite-size scaling of the entanglement entropy of a block of the first l consecutive sites in a chain with open boundary conditions and length L is

$$\mathcal{S}(l, L) = \frac{c}{6}W + b', \quad (3)$$

where c is the central charge of the corresponding CFT, b' is a non-universal constant and W is a function of both L and l : $W(l, L) = \ln \left[\frac{2L}{\pi} \sin(\pi l/L) \right]$ [49–51].

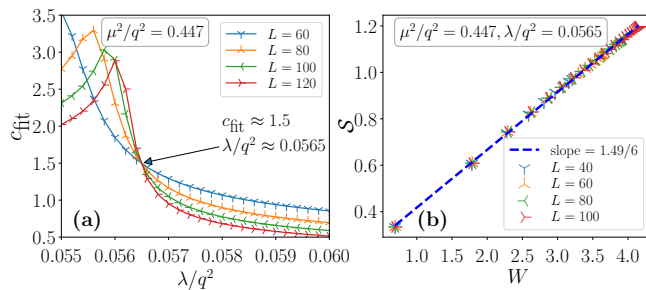


FIG. 2. Entropy scaling of the AHM₂. (a) The fitted central charge c_{fit} according to (3) for fixed $\mu^2/q^2 = 0.447$ and different system sizes. Curves for different system-sizes crosses each other at $\lambda/q^2 \approx 0.0565$ and $c_{\text{fit}} \approx 3/2$. (b) The scaling of the entanglement entropy at the critical point for different system sizes yields the central charge of the critical theory as $c = 1.49(1)$.

As discussed in [52, 53], we can accurately pin-point the SOQPT by adapting the idea of the phenomenological renormalization group [54] to the scaling of the entropy in (3). In particular, we expect that at the critical point, there should be a value of c independent of the system's size. As a result, for each system size L we obtain c_{fit} by fitting (3) to our numerical data for $\mathcal{S}(l, L)$. The extracted values in the $(\mu^2/q^2, \lambda/q^2)$ -plane depend on L and become independent of the system size only at the critical point. Our data suggest that the L dependent central charges collapse to a single value at $(\mu^2/q^2 = 0.447(1), \lambda/q^2 = 0.0565(1))$ (see Fig. 2(a)). Moreover, the central charge at the critical point $(\mu_c^2/q^2 = 0.447, \lambda_c/q^2 = 0.0565)$ is found to be $c = 1.49(1)$ (Fig. 2(b)) [55].

A value of the central charge above one suggests that we are not dealing with a minimal model. However, we want to argue here that we are in the presence of the direct sum of two different minimal models, each contributing to a piece of the total central charge, a $c_f = 1/2$ for a free Majorana fermion and a $c_b = 1$ for free boson. This scenario is strongly motivated by the standard Higgs mechanism. The complex Higgs field separates into its

amplitude and its phase. The amplitude mode is effectively described by a real $\lambda\phi^4$ theory that undergoes the standard Ising phase transition (the $c = 1/2$ part). The phase, on the other hand, provides the longitudinal degree of freedom to the photon field. The latter at the transition becomes massless and provides the $c = 1$ free bosonic part of the spectrum. The value of $c = 1.5$ furthermore strongly suggests, based on the c theorem, that the two parts should be non-interacting [56].

In order to confirm this scenario we compute the entanglement spectrum that is also known to encode the central charge of the theory [57]. The entanglement spectrum, denoted by ε_s , is the spectrum of the entanglement Hamiltonian $H_l = -\log(\rho_l)$. By assuming a factorized ground state, we should observe that the smallest eigenvalue of H_l , ε_0 should diverge logarithmically. In particular using the CFT analysis of [57] we should see that

$$\varepsilon_0 = \left(\varepsilon_0^{\text{Ising}} + \varepsilon_0^{\text{boson}} \right) \propto \frac{(c_f + c_b)}{12} W + O(1/W). \quad (4)$$

By fitting our numerical data to Eq. (4), once more we observe perfect collapse on the functional form predicted by the CFT, but the numerical result for $c_{\text{eff}} = 1.20(1)$ is not compatible with the value 1.5 (see Fig. 3(a)). This disagreement between the scaling of the entanglement entropy and that for the entanglement ground state already suggests that the critical point is unusual and exotic in nature.

We thus turn to analyze the operator content of the model by studying the correlation functions of local operators. We should be able to identify a set of primary operators, by studying the large distance two point correlations function that should decay algebraically as $\phi(0)\phi(r) \sim 1/r^{\Delta_\phi}$. The presence of gauge symmetry, however, strongly reduces the set of operators we can consider. It indeed implies that most of the candidate observables that should couple to primary operators are either trivial (due to the low-dimensionality of the system) or vanishing since they are not gauge invariant. The only non-vanishing operators are indeed Wilson lines terminating on a boson anti-boson pair, and electric field correlations. We also have access to local operators such as $\hat{\phi}^\dagger\hat{\phi}$ and $\hat{\Pi}^\dagger\hat{\Pi}$ that couple both to the real part and the phase of the field. By assuming we are dealing with a CFT, we can also use the conformal map that maps the profile of local operators to two points correlation functions on the full plane (see e.g. [58]).

At first we analyze the behavior of $\langle \hat{L}_l^2 \rangle$ as function of the chord coordinate W . The numerical results, presented in Fig. 3(b), show that $\langle \hat{L}_l^2 \rangle$ diverges logarithmically as a function of W , unveiling that \hat{L}^2 behaves as a free-bosonic field. Furthermore, the constant in front of the logarithmic divergence is 0.10(1). Assuming it is $c/12$ we get an estimate for the central charge $c = 1.2(1)$. It coincides with the one extracted from the scaling of

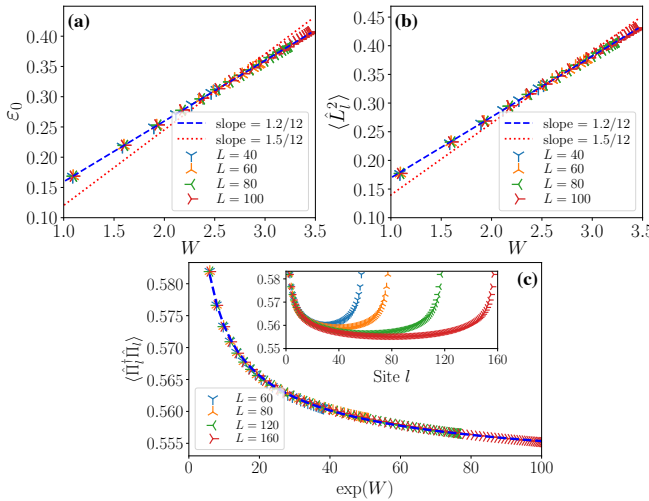


FIG. 3. (a) The scaling of the entanglement ground state ε_0 matches perfectly the functional form suggested by the CFT analysis, reported in the text. However, the numerical value for the central charge deviates by around the 20% from the value we extract by studying the scaling of the entanglement entropy as the best fit suggests $c_{\text{eff}} = 1.20(1)$. (b) The scaling of $\langle \hat{L}_l^2 \rangle$ also matches perfectly the functional form suggested by the CFT analysis. From the pre-factor, we can infer a value of the central charge, $c_{\text{eff}} = 1.2(1)$ as in the case of ε_0 . In (a) and (b) the red-dotted lines assume $c = 1.5$ and clearly deviate from our numerical result. (c) The scaling of $\langle \hat{\Pi}_l^\dagger \hat{\Pi}_l \rangle$ according to the CFT prediction reported in the main text (Eq. (5)). It couples both to the identity operator and one primary with scaling dimension Δ that comes out to be $\Delta = 0.51(2)$ from the fit.

the entanglement ground state, and differs from the one extracted from the entanglement entropy.

Turning to analyzing the profile of $\langle \hat{\Pi}_l^\dagger \hat{\Pi}_l \rangle$ as a function of W we find that

$$\langle \hat{\Pi}_l^\dagger \hat{\Pi}_l \rangle \simeq a + b(\exp(W))^{-\Delta}, \quad (5)$$

where a and b encode the overlap of the above expectation value with the identity operator and one of the primaries. The numerical data reported in Fig. 3(c) seem to suggest that $\Delta \simeq 0.5$, the conjugate operator to the one that would match to the derivative of the electric field.

Unfortunately, we do not find any operator that couples to the primary of the Ising part of the CFT. Summarizing, our data seem to confirm that we have one part of the system that behaves as free boson and suggest that $\partial_x \hat{L}^2$ should have a large overlap with the primary operator (the derivative of the free bosonic field), while $\hat{\Pi}^\dagger \hat{\Pi}$ should have a strong overlap with the conjugate primary operator.

Now moving away from the critical point ($\mu_c^2/\lambda_c = 0.447/0.0565$), we can use the standard scaling hypothesis to extract the exponent ν from the collapse of the

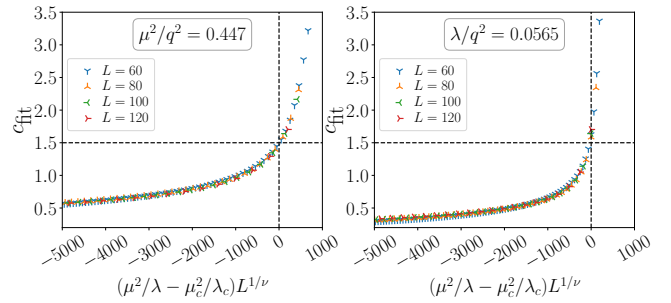


FIG. 4. The collapse of c_{fit} according to the scaling hypothesis (6) in the neighborhood of the critical point $\mu_c^2/\lambda_c = 0.447/0.0565$ for fixed $\mu^2/q^2 = 0.447$ (left) and for fixed $\lambda/q^2 = 0.0565$ (right). In both the cases, the critical exponent is found to be $\nu = 0.5 \pm 0.02$ from data collapses.

fitted central charge as

$$c_{\text{fit}}(L) = f \left((\mu^2/\lambda - \mu_c^2/\lambda_c)L^{1/\nu} \right), \quad (6)$$

where $f(\cdot)$ is a continuous function and ν is the corresponding critical exponent. After performing data collapse according to (6) in the neighborhood of the critical point μ_c^2/λ_c (see Fig. 4) we find the critical exponent to be $\nu = 1/2 \pm 0.02$ that matches the value observed in the transition from polarized to critical phase in the XX model in a magnetic field [59–61]. The same transition can be understood in terms of free bosons that pass from their Fock vacuum to the superfluid regime as the chemical potential exceeds the width of the first band. In our case, the strange thing is that there is no superfluid regime, but just a single critical point where the gauge-boson condense, while away from the critical point our system passes from vacuum to a Mott insulator phase. Now using the standard scaling hypothesis, once we have figured out that $\nu = 1/2$ we can deduce that $\langle \hat{\Pi}^\dagger \hat{\Pi} \rangle \simeq (\mu^2/\lambda - \mu_c^2/\lambda_c)$, meaning that $\beta = 1$.

It is worth pointing out that $\nu = 1/2$, seems inconsistent with a CFT, where we would expect, that $d - 1/\nu = \Delta$ with Δ the thermal critical exponent and d being 2 for the 1+1D quantum system, while we find $d - 1/\nu = 0$. However, all our results so far have been obtained by assuming a full conformal invariance in mapping the correlation function of our finite system to the ones of an infinite plane by means of a conformal transformations.

The appearance of $\nu = 1/2$, together with the failure to identify a local operator that couples to the primary field of the Ising part of the CFT, contrasts with the factorization on the critical point. However, by repeating a similar analysis in a \mathbb{Z}_3 gauge theory coupled to bosonic matter we find a $c \simeq 0.8 + 0.5$ [62]. As a result we still believe that the factorization hypothesis is correct, but it requires further analysis to be appropriately confirmed.

Discussion and Conclusions.— In this paper we have analyzed the phase diagram of the AHM on a discrete lat-

tice in 1+1D. We have shown that on the lattice there are two distinct regions, the confined and the Higgs regions that are separated by line of FOQPT that terminates in a SOQPT. Beyond the SOQPT the two regions are connected by a smooth crossover. The presence of a SOQPT allows one to construct an unorthodox continuum limit of the theory that should be described by free fermions and free bosons that do not interact.

This would result in a CFT with central charge $c = 3/2$, compatible with our numerical result and would have a compelling interpretation in terms of the standard Higgs mechanism – the real part of the complex field undergoes an Ising transition (the $c = 1/2$ part), while the phase of it provides the transverse degree of freedom to the photon that becomes dynamical and massless (the $c = 1$ part).

However, further numerical analysis unveils also surprising pieces of the puzzle that do not fit in our interpretation. For example, we did not find a local operator that couples to the $c = 1/2$ part of the CFT. The scaling of the entanglement ground state of the system should follow a similar law to the one of the entanglement entropy. The numerical value of the central charge that we extract from it is $c = 1.20(1)$, the same that we extract from the logarithmic divergence of the \hat{L}^2 operator. We also obtain $\nu = 1/2$ analyzing the collapse of the data for the entanglement entropy close to the critical point, in contrast to the expected $\nu = 1$.

Are we actually observing a Lorentz invariant critical point [41] where the Higgs and photon mode factorize? We strongly believe this is the case, though there are still some unanswered questions in our study. We strongly believe that our paper will open the debate, and that together with the broader scientific community we will soon have a final picture of the mechanism behind this newly observed critical point.

We are grateful to Marcello Dalmonte for the valuable suggestion regarding the analysis of the sound velocity. T.C. thanks Subhroneel Chakrabarti for useful discussions. L.T. would like to acknowledge the discussions with F. Gliozzi, B. Fiol, and E. Vicari on the topics presented. The numerical computations have been possible thanks to PL-Grid Infrastructure. This research has been supported by National Science Centre (Poland) under project 2017/25/Z/ST2/03029 (T.C. and J.Z.). M.L. acknowledges support from ERC AdG NOQIA, State Research Agency AEI (“Severo Ochoa” Center of Excellence CEX2019-000910-S, Plan National FIDEUA PID2019-106901GB-I00/10.13039 / 501100011033, FPI, QUANTERA MAQS PCI2019-111828-2 / 10.13039/501100011033), Fundació Privada Cellex, Fundació Mir-Puig, Generalitat de Catalunya (AGAUR Grant No. 2017 SGR 1341, CERCA program, QuantumCAT U16-011424, co-funded by ERDF Operational Program of Catalonia 2014-2020), EU Horizon 2020 FET-OPEN OPTOLogic (Grant No.

899794), and the National Science Centre, Poland (Symfonia Grant No. 2016/20/W/ST4/00314), Marie Skłodowska-Curie grant STRETCH No. 101029393, “La Caixa” Junior Leaders fellowships (ID100010434), and EU Horizon 2020 under Marie Skłodowska-Curie grant agreement No 847648 (LCF/BQ/PI19/11690013, LCF/BQ/PI20/11760031, LCF/BQ/PR20/11770012). L.T. acknowledges support from the Ramón y Cajal program RYC-2016-20594, the “Plan Nacional Generación de Conocimiento” PGC2018-095862-B-C22 and the State Agency for Research of the Spanish Ministry of Science and Innovation through the “Unit of Excellence María de Maeztu 2020-2023” award to the Institute of Cosmos Sciences (CEX2019-000918-M).

* titas.chanda@uj.edu.pl

- [1] C. Borgs and F. Nill, The phase diagram of the Abelian lattice Higgs model. A review of rigorous results, *Journal of Statistical Physics* **47**, 877 (1987).
- [2] D. Brydges, J. Fröhlich, and E. Seiler, Diamagnetic and critical properties of Higgs lattice gauge theories, *Nuclear Physics B* **152**, 521 (1979).
- [3] T. Chanda, J. Zakrzewski, M. Lewenstein, and L. Tagliacozzo, Confinement and Lack of Thermalization after Quenches in the Bosonic Schwinger Model, *Phys. Rev. Lett.* **124**, 180602 (2020).
- [4] J. Schwinger, On gauge invariance and vacuum polarization, *Phys. Rev.* **82**, 664 (1951).
- [5] J. Schwinger, Gauge Invariance and Mass, *Phys. Rev.* **125**, 397 (1962).
- [6] J. Schwinger, Gauge Invariance and Mass. II, *Phys. Rev.* **128**, 2425 (1962).
- [7] S. Coleman, More about the massive Schwinger model, *Annals of Physics* **101**, 239 (1976).
- [8] P. W. Anderson, Plasmons, gauge invariance, and mass, *Phys. Rev.* **130**, 439 (1963).
- [9] F. Englert and R. Brout, Broken symmetry and the mass of gauge vector mesons, *Phys. Rev. Lett.* **13**, 321 (1964).
- [10] P. W. Higgs, Broken symmetries and the masses of gauge bosons, *Phys. Rev. Lett.* **13**, 508 (1964).
- [11] G. S. Guralnik, C. R. Hagen, and T. W. B. Kibble, Global conservation laws and massless particles, *Phys. Rev. Lett.* **13**, 585 (1964).
- [12] M. E. Peskin and D. V. Schroeder, *An introduction to quantum field theory* (Addison-Wesley Pub. Co, Reading, Mass, 1995).
- [13] S. Coleman, *Aspects of Symmetry: Selected Erice Lectures* (Cambridge University Press, 1985).
- [14] Z. Komargodski, A. Sharon, R. Thorngren, and X. Zhou, Comments on Abelian Higgs Models and Persistent Order, *SciPost Phys.* **6**, 3 (2019).
- [15] D. Tong, Lectures on Gauge Theory, <https://www.damtp.cam.ac.uk/user/tong/gaugetheory.html>.
- [16] E. Fradkin and S. H. Shenker, Phase diagrams of lattice gauge theories with Higgs fields, *Phys. Rev. D* **19**, 3682 (1979).
- [17] D. J. E. Callaway and L. J. Carson, Abelian Higgs model: A Monte Carlo study, *Phys. Rev. D* **25**, 531 (1982).

[18] O. Dutta, L. Tagliacozzo, M. Lewenstein, and J. Zakrzewski, Toolbox for abelian lattice gauge theories with synthetic matter, *Phys. Rev. A* **95**, 053608 (2017).

[19] C. Schweizer, F. Grusdt, M. Berngruber, L. Barbiero, E. Demler, N. Goldman, I. Bloch, and M. Aidelsburger, Floquet approach to \mathbb{Z}_2 lattice gauge theories with ultracold atoms in optical lattices, *Nature Physics* **15**, 1168 (2019).

[20] F. Görg, K. Sandholzer, J. Minguzzi, R. Desbuquois, M. Messer, and T. Esslinger, Realization of density-dependent Peierls phases to engineer quantized gauge fields coupled to ultracold matter, *Nature Physics* **15**, 1161 (2019).

[21] A. Mil, T. V. Zache, A. Hegde, A. Xia, R. P. Bhatt, M. K. Oberthaler, P. Hauke, J. Berges, and F. Jendrzejewski, A scalable realization of local U(1) gauge invariance in cold atomic mixtures, *Science* **367**, 1128 (2020).

[22] M. C. Bañuls, R. Blatt, J. Catani, A. Celi, J. I. Cirac, M. Dalmonte, L. Fallani, K. Jansen, M. Lewenstein, S. Montangero, *et al.*, Simulating lattice gauge theories within quantum technologies, *Eur. Phys. J. D* **74**, 165 (2020).

[23] M. Aidelsburger, L. Barbiero, A. Bermudez, T. Chanda, A. Dauphin, D. González-Cuadra, P. R. Grzybowski, S. Hands, F. Jendrzejewski, J. Jünemann, G. Juzeliunas, V. Kasper, A. Piga, S.-J. Ran, M. Rizzi, G. Sierra, L. Tagliacozzo, E. Tirrito, T. V. Zache, J. Zakrzewski, E. Zohar, and M. Lewenstein, Cold atoms meet lattice gauge theory, [arXiv:2106.03063](https://arxiv.org/abs/2106.03063).

[24] K. Kasamatsu, I. Ichinose, and T. Matsui, Atomic Quantum Simulation of the Lattice Gauge-Higgs Model: Higgs Couplings and Emergence of Exact Local Gauge Symmetry, *Phys. Rev. Lett.* **111**, 115303 (2013).

[25] Y. Kuno, S. Sakane, K. Kasamatsu, I. Ichinose, and T. Matsui, Quantum simulation of (1 + 1)-dimensional U(1) gauge-Higgs model on a lattice by cold Bose gases, *Phys. Rev. D* **95**, 094507 (2017).

[26] D. González-Cuadra, E. Zohar, and J. I. Cirac, Quantum simulation of the Abelian-Higgs lattice gauge theory with ultracold atoms, *New Journal of Physics* **19**, 063038 (2017).

[27] J. Zhang, J. Unmuth-Yockey, J. Zeiher, A. Bazavov, S.-W. Tsai, and Y. Meurice, Quantum Simulation of the Universal Features of the Polyakov Loop, *Phys. Rev. Lett.* **121**, 223201 (2018).

[28] J. Unmuth-Yockey, J. Zhang, A. Bazavov, Y. Meurice, and S.-W. Tsai, Universal features of the Abelian Polyakov loop in 1 + 1 dimensions, *Phys. Rev. D* **98**, 094511 (2018).

[29] J. Park, Y. Kuno, and I. Ichinose, Glassy dynamics from quark confinement: Atomic quantum simulation of the gauge-Higgs model on a lattice, *Phys. Rev. A* **100**, 013629 (2019).

[30] Y. Meurice, Theoretical methods to design and test quantum simulators for the compact Abelian Higgs model, [arXiv:2107.11366](https://arxiv.org/abs/2107.11366).

[31] D. Pekker and C. Varma, Amplitude/Higgs Modes in Condensed Matter Physics, *Annual Review of Condensed Matter Physics* **6**, 269 (2015).

[32] C. Schori, T. Stöferle, H. Moritz, M. Köhl, and T. Esslinger, Excitations of a Superfluid in a Three-Dimensional Optical Lattice, *Phys. Rev. Lett.* **93**, 240402 (2004).

[33] T. Stöferle, H. Moritz, C. Schori, M. Köhl, and T. Esslinger, Transition from a Strongly Interacting 1D Superfluid to a Mott Insulator, *Phys. Rev. Lett.* **92**, 130403 (2004).

[34] M. Endres, T. Fukuhara, D. Pekker, M. Cheneau, P. Schauß, C. Gross, E. Demler, S. Kuhr, and I. Bloch, The ‘Higgs’ Amplitude Mode at the Two-Dimensional Superfluid/Mott Insulator Transition, *Nature* **487**, 454 (2012).

[35] T. D. Kühner and H. Monien, Phases of the one-dimensional Bose-Hubbard model, *Phys. Rev. B* **58**, R14741 (1998).

[36] I. Danshita and A. Polkovnikov, Superfluid-to-Mott-insulator transition in the one-dimensional Bose-Hubbard model for arbitrary integer filling factors, *Phys. Rev. A* **84**, 063637 (2011).

[37] M. A. Cazalilla, R. Citro, T. Giamarchi, E. Orignac, and M. Rigol, One dimensional bosons: From condensed matter systems to ultracold gases, *Rev. Mod. Phys.* **83**, 1405 (2011).

[38] O. Dutta, M. Gajda, P. Hauke, M. Lewenstein, D.-S. Lühmann, B. A. Malomed, T. Sowiński, and J. Zakrzewski, Non-standard Hubbard models in optical lattices: a review, *Reports on Progress in Physics* **78**, 066001 (2015).

[39] U. Schollwöck, The density-matrix renormalization group in the age of matrix product states, *Annals of Physics* **326**, 96 (2011).

[40] R. Orús, A practical introduction to tensor networks: Matrix product states and projected entangled pair states, *Annals of Physics* **349**, 117 (2014).

[41] See supplementary material, that includes Refs. [63–65], for the derivation of the lattice Hamiltonian and for the convincing evidence towards Lorentz invariance of the critical point mentioned in the main text.

[42] The operators are defined as

$$\hat{\phi}_j = \frac{1}{\sqrt{2}} (\hat{a}_j + \hat{b}_j^\dagger), \quad \hat{\Pi}_j = \frac{i}{\sqrt{2}} (\hat{a}_j^\dagger - \hat{b}_j),$$

$$\hat{\phi}_j^\dagger = \frac{1}{\sqrt{2}} (\hat{a}_j^\dagger + \hat{b}_j), \quad \hat{\Pi}_j^\dagger = \frac{i}{\sqrt{2}} (\hat{b}_j^\dagger - \hat{a}_j),$$

as discussed in e.g. [3].

[43] S. R. White, Density matrix formulation for quantum renormalization groups, *Phys. Rev. Lett.* **69**, 2863 (1992).

[44] S. R. White, Density-matrix algorithms for quantum renormalization groups, *Phys. Rev. B* **48**, 10345 (1993).

[45] S. R. White, Density matrix renormalization group algorithms with a single center site, *Phys. Rev. B* **72**, 180403 (2005).

[46] U. Schollwöck, The density-matrix renormalization group, *Rev. Mod. Phys.* **77**, 259 (2005).

[47] We have checked that the results do not depend significantly on this cutoff, by repeating the simulations for maximum boson occupancy from 6 to 15.

[48] To confirm about the Lorentz invariance of the critical point, we calculate the ‘sound velocity’ from the ground state energy scaling as in [66–69]. For details see [41].

[49] C. Callan and F. Wilczek, On geometric entropy, *Physics Letters B* **333**, 55 (1994).

[50] G. Vidal, J. I. Latorre, E. Rico, and A. Kitaev, Entanglement in Quantum Critical Phenomena, *Phys. Rev. Lett.* **90**, 227902 (2003).

[51] P. Calabrese and J. Cardy, Entanglement entropy and quantum field theory, *Journal of Statistical Mechanics* **2004** (06), P06002.

[52] T. Koffel, M. Lewenstein, and L. Tagliacozzo, Entanglement Entropy for the Long-Range Ising Chain in a Transverse Field, *Phys. Rev. Lett.* **109**, 267203 (2012).

[53] A. S. Buyskikh, L. Tagliacozzo, D. Schuricht, C. A. Hoooley, D. Pekker, and A. J. Daley, Spin models, dynamics, and criticality with atoms in tilted optical superlattices, *Phys. Rev. Lett.* **123**, 090401 (2019).

[54] M. P. Nightingale, Scaling theory and finite systems, *Physica A* **83**, 561 (1975).

[55] It is important to notice that our analysis is based on the full scaling form of the entropy in (3) that holds for conformally invariant systems only. The logarithmic divergence of the half chain entropy on the other hand can be observed also for systems that only posses scale invariance [52, 70, 71].

[56] A. B. Zomolodchikov, “Irreversibility” of the flux of the renormalization group in a 2D field theory, *Soviet Journal of Experimental and Theoretical Physics Letters* **43**, 730 (1986).

[57] J. Cardy and E. Tonni, Entanglement Hamiltonians in two-dimensional conformal field theory, *Journal of Statistical Mechanics* **2016** (12), 123103.

[58] Introduction to theory of finite-size scaling, in *Finite-Size Scaling*, Current Physics–Sources and Comments, Vol. 2, edited by J. L. Cardy (Elsevier, 1988) pp. 1–7.

[59] J. Latorre, E. Rico, and G. Vidal, Ground state entanglement in quantum spin chains, *Quantum Information and Computation* **4**, 48 (2004).

[60] M. Campostrini and E. Vicari, Quantum critical behavior and trap-size scaling of trapped bosons in a one-dimensional optical lattice, *Phys. Rev. A* **81**, 063614 (2010).

[61] A. Dutta, G. Aeppli, B. K. Chakrabarti, U. Divakaran, T. F. Rosenbaum, and D. Sen, *Quantum Phase Transitions in Transverse Field Spin Models: From Statistical Physics to Quantum Information* (Cambridge University Press, 2015).

[62] T. Chanda, M. Lewenstein, J. Zakrzewski, and L. Tagliacozzo, *in preparation*.

[63] H. W. J. Blöte, J. L. Cardy, and M. P. Nightingale, Conformal invariance, the central charge, and universal finite-size amplitudes at criticality, *Phys. Rev. Lett.* **56**, 742 (1986).

[64] I. Affleck, Universal term in the free energy at a critical point and the conformal anomaly, *Phys. Rev. Lett.* **56**, 746 (1986).

[65] I. Affleck, D. Gepner, H. J. Schulz, and T. Ziman, Critical behaviour of spin- s heisenberg antiferromagnetic chains: analytic and numerical results, *Journal of Physics A: Mathematical and General* **22**, 511 (1989).

[66] K. Hallberg, X. Q. G. Wang, P. Horsch, and A. Moreo, Critical Behavior of the $S = 3/2$ Antiferromagnetic Heisenberg Chain, *Phys. Rev. Lett.* **76**, 4955 (1996).

[67] J. C. Xavier, Entanglement entropy, conformal invariance, and the critical behavior of the anisotropic spin- s Heisenberg chains: DMRG study, *Phys. Rev. B* **81**, 224404 (2010).

[68] M. Dalmonte, E. Ercolessi, and L. Taddia, Critical properties and Rényi entropies of the spin- $\frac{3}{2}$ XXZ chain, *Phys. Rev. B* **85**, 165112 (2012).

[69] N. Chepiga and F. Mila, Excitation spectrum and density matrix renormalization group iterations, *Phys. Rev. B* **96**, 054425 (2017).

[70] G. Refael and J. E. Moore, Entanglement Entropy of Random Quantum Critical Points in One Dimension, *Phys. Rev. Lett.* **93**, 260602 (2004).

[71] J. I. Latorre, R. Orús, E. Rico, and J. Vidal, Entanglement entropy in the Lipkin-Meshkov-Glick model, *Phys. Rev. A* **71**, 064101 (2005).

Supplementary material: From the continuum to the lattice

The Lagrangian density of the Abelian-Higgs model is given by [12, 15]

$$\mathcal{L} = -[D_\mu \phi]^* D^\mu \phi - \frac{1}{4} F_{\mu\nu} F^{\mu\nu} - V(\phi), \quad (7)$$

with

$$V(\phi) = -\mu^2 |\phi|^2 + \frac{\lambda}{2} |\phi|^4. \quad (8)$$

Here ϕ is the complex scalar field, $D_\mu = (\partial_\mu + iqA_\mu)$ is the covariant derivative with q and A_μ being the gauge coupling and the electromagnetic vector potential respectively, and $F_{\mu\nu} = \partial_\mu A_\nu - \partial_\nu A_\mu$ is the electromagnetic field tensor. Here, we use the metric convection $(-1, 1, 1, 1)$ or $(-1, 1)$ (in 1+1 dimension).

For $\mu^2 < 0$, the system describes the bosonic Schwinger model (BSM) [3] with added $|\phi|^4$ -interaction, while $\mu^2 > 0$ describes Abelian-Higgs model (AHM) where the potential attains minimum ($V_{\min} = -\frac{\mu^4}{2\lambda}$) at non-zero value of the field-strength $|\phi_0| = \sqrt{\mu^2/\lambda}$, describing spontaneous symmetry breaking at semiclassical level.

After fixing the temporal gauge $A_t(x, t) = 0$, we get the quantum 1+1D Hamiltonian in the continuum as

$$\hat{H} = \int dx \left[\hat{\Pi}^\dagger(x) \hat{\Pi}(x) - \mu^2 \hat{\phi}^\dagger(x) \hat{\phi}(x) + \frac{\lambda}{2} (\hat{\phi}^\dagger(x))^2 (\hat{\phi}(x))^2 + \frac{1}{2} \hat{E}_x^2(x) + (\partial_x - iq\hat{A}_x(x)) \hat{\phi}^\dagger(x) (\partial_x + iq\hat{A}_x(x)) \hat{\phi}(x) \right], \quad (9)$$

where $\hat{E}_x(x)$, $\hat{\Pi}(x)$, and $\hat{\Pi}^\dagger(x)$ are the canonical conjugate operators corresponding to $\hat{A}_x(x)$, $\hat{\phi}(x)$, and $\hat{\phi}^\dagger(x)$ respectively, satisfying the canonical commutation relations:

$$\begin{aligned} [\hat{A}_x(x_1), \hat{E}_x(x_2)] &= [\hat{\phi}(x_1), \hat{\Pi}(x_2)] \\ &= [\hat{\phi}^\dagger(x_1), \hat{\Pi}^\dagger(x_2)] = i\delta(x_1 - x_2). \end{aligned} \quad (10)$$

Note: The quantization of the $|\phi|^4$ term may be done in various manners. Here we do not enforce any normal ordering but rather take $|\phi|^4 \xrightarrow{\text{quantization}} (\phi^\dagger)^2 \phi^2$.

Following [3], we can straightforwardly discretize the above Hamiltonian on a 1D spatial lattice with the lattice spacing a , and we ultimately arrive at the Hamiltonian (1) in the main text.

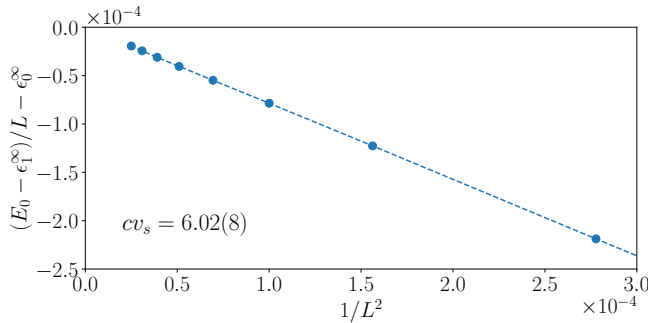


FIG. 5. Finite-size scaling of the ground state energy E_0 at the critical point according to Eq. (11) that gives the sound velocity $v_s \simeq 4$.

Supplementary material: Evidence for Lorentz invariance of the critical point

In the main text, the analysis of the critical point ($\mu_c^2/q^2 = 0.447$, $\lambda_c/q^2 = 0.0565$) by means of the predictions from conformal field theory (CFT) have been done

assuming Lorentz invariance of the critical point. To verify this assumption, we calculate the “sound velocity” at the critical point from the scaling of ground state energy. For a Lorentz invariant system with open boundary condition (OBC) having linear dispersion at low energies, the ground state energy E_0 scales with system size L as [63–65]

$$E_0(L) = \epsilon_0^\infty L + \epsilon_1^\infty - \frac{\pi c v_s}{24L}, \quad (11)$$

where ϵ_0^∞ is the ground state energy density in the bulk and ϵ_1^∞ is the surface free energy in the thermodynamic limit, c is the central charge of the corresponding CFT, and v_s is the sound velocity. For a Lorentz invariant system v_s must be non-zero, while it vanishes for Lorentz non-invariant critical points with a quadratic dispersion.

To estimate v_s , we perform the finite-size scaling of the ground state energy according to Eq. (11) at the critical point (for similar analysis, see [66–69]). Such a finite-size scaling (Fig. 5) yields $cv_s = 6.02 \pm 0.08$ ($v_s \simeq 4$ for $c = 1.5$), confirming the Lorentz invariance of the critical point analyzed in the main text.